Energy Conversion and Management xxx (2016) xxx–xxx

Contents lists available at ScienceDirect

Energy Conversion and Management

journal homepage: www.elsevier.com/locate/enconman

Exergy analysis of a Combined Cooling, Heating and Power system integrated with wind turbine and compressed air energy storage system

Amin Mohammadi [a], Mohammad H. Ahmadi [b,*], Mokhtar Bidi [a,*], Fatemeh Joda [a], Antonio Valero [c], Sergio Uson [c]

[a] Faculty of Mechanical & Energy Engineering, Shahid Beheshti University, A.C., Tehran, Iran
[b] Department of Renewable Energies, Faculty of New Sciences and Technologies, University of Tehran, Tehran, Iran
[c] CIRCE, Center of Research for Energy Resources and Consumption, Universidad de Zaragoza, Mariano Esquillor n. 15, 50018 Zaragoza, Spain

ARTICLE INFO

Article history:
Received 2 August 2016
Received in revised form 24 October 2016
Accepted 1 November 2016
Available online xxxx

Keywords:
CCHP
Wind energy
Compressed air energy storage
ORC
Absorption chiller
Exergy

ABSTRACT

Utilizing renewable energies is the promising solution to the environmental problems which are brought about due to fossil fuel consumption. The fact that these kinds of energies are intermittent can be overcome with using energy storage systems. Wind energy coupled with compressed air energy storage systems is one of the best candidates in this respect. The main objective of this paper is to study the integration of this system with a Combined Cooling, Heating and Power cycle comprised of a gas turbine, an organic Rankine cycle and an absorption refrigeration system. Energy and exergy analyses are applied to the system and the effect of key parameters on the system performance are analyzed. The results show that under design condition, the system can generate 33.67 kW electricity, 2.56 kW cooling and 1.82 ton per day hot water with a round trip energy efficiency of 53.94%. Also exergy analysis reveals that wind turbine, combustion chamber and compress air storage system have the highest amount of exergy destruction respectively. Finally, sensitivity analysis shows that parameters related to gas turbine are the most prominent parameters of the system which can change performance of the system considerably.

1. Introduction

During the last two centuries, energy consumption has increased rapidly due to population growth and technology improvements. Based on data published by DOE [1], almost 16% of total energy is consumed in residential and commercial sectors for cooling, heating and lighting purposes. Consumption of this amount of energy has many consequences, on the top of them environmental and economic problems. Combined cooling, heating and power (CCHP) systems are the promising solution to reduce energy consumption in these sectors [2].These systems also reduce energy losses in energy transmission system.

Many researchers have studied CCHP systems. Hanafizadeh et al. [3] defined three different scenarios for a CCHP system in an office building with different prime movers and studied them economically and environmentally. Chen et al. [4] studied coupling of a CCHP based on PEM fuel cell and absorption refrigeration system in steady state. They showed that efficiency of the system can reach to70.1% in summer and 82% in winter. Ma et al. [5] coupled an ammonia-water mixture with a SOFC-GT system and evaluated performance of the total system. They showed that the proposed system can reach to thermal efficiencies higher than 80%. Zhao et al. [6] analyzed a cascade system which is comprised of a SOFC, a gas turbine, a steam turbine and a Li-Br absorption refrigeration cycle to provide simultaneous power, heat and cooling. They also performed a sensitivity analysis on the most important parameters of the system. Li and Hu [7] performed exergetic comparison between an absorption refrigeration system and an electric compression chiller in a CCHP system which uses a combined cycle of gas turbine and steam turbine as prime mover. They showed that the selection between these two types of refrigeration is heavily dependent on the distance between the power station and refrigeration system, in a way that when the distance is lower than 5 km, absorption refrigeration system is more effective. Ebrahimi et al. [8] performed exergy analysis on a CCHP system which uses a steam and air heat exchanger to provide heating and a steam ejector condenser to provide cooling. They also optimized the plants performance using genetic algorithm. Gao et al. [9] analyzed the effect of gas composition on the performance of a gas engine which drives a CCHP system. They performed their study under both design and off-design conditions. Chen et al. [10] carried

* Corresponding authors.
E-mail addresses: mohammadhosein.ahmadi@gmail.com (M.H. Ahmadi), m_bidi@sbu.ac.ir (M. Bidi).

http://dx.doi.org/10.1016/j.enconman.2016.11.003
0196-8904/

Nomenclature

A	area (m^2)
COP	coefficient of performance
c_p	power coefficient
C_p	specific heat at constant pressure (kJ/kg K)
Ex	exergy (kW)
ex	specific exergy (kJ/kg)
h	specific enthalpy (kJ/kg)
LHV	lower heating value (kJ/kg)
$\dot{m}$	mass flow rate (kg/s)
$\dot{Q}$	heat (kW)
r_p	pressure ratio
R_p	total pressure ratio of compression train
RTE	round trip efficiency (%)
s	specific entropy (kJ/kg K)
T	temperature (C)
t	time (h)
V	volume (m^3)
$\dot{W}$	power (kW)
x	mass fraction
y	molar fraction

Greek symbols

γ	specific heat ratio
η	efficiency (%)
ξ	chemical exergy/energy ratio
ρ	density (kg/m^3)
υ	velocity (m/s)
ε	effectiveness (%)

Subscripts

a	Air
CC	combustion chamber
ch	chemical
comp	compressor
f	fuel
g	flue gas
GT	gas turbine
ph	physical
tur	turbine
w	water
WT	wind turbine

out energy and exergy analyses on a CCHP system including a micro gas turbine and an absorption chiller. They also added a heat exchanger to produce hot water from gas turbine exhaust flow. Moya et al. [11] carried out an experimental analysis on a CCHP system consisting of a micro gas turbine, an air cooled absorption chiller and a heat exchanger to compute its efficiency. They also performed economic analysis to analyze feasibility of the system. Ochoa et al. [12] performed energy and exergy analyses on a cogeneration system consist of a micro turbine, single-effect LiBr/H2O absorption chiller and a heat exchanger. They showed that energy and exergy efficiency of the system are equal to 50% and 26%. Yang et al. [13] studied off-design performance of a CCHP system driven by gas turbine and discussed different definitions of CCHP efficiencies. Kong et al. [14] used linear programming to find out the optimal strategy for minimizing total cost of energy in CCHP systems. They showed that the optimal solution is heavily dependent on the load conditions.

One of the problems of using gas turbines is that their outlet temperature is high and this leads to a huge energy loss. Utilizing a bottom cycle to recover this energy can considerably boost the system efficiency. ORC cycles are good candidates for this purpose due to their low critical temperature. Borunda et al. [15] proposed a novel configuration for coupling ORC and parabolic trough collector. They used the proposed cycle for providing energy in a textile factory as a CHP system. They showed that using this configuration, the size of the thermal storage could be reduced. Pantaleo et al. [16] performed a techno-economic comparison between a gas turbine and a steam turbine as top cycle for a CHP system. To increase performance, they coupled an ORC cycle to both of these cycles. Fang et al. [17] proposed a new configuration of CCHP-ORC system which has the capability of adjusting electricity to thermal energy output ratio through changing electric chiller and ORC system load. Javan et al. [18] used an ORC cycle, an ejector refrigerator system and a water heater as a CCHP system to recover waste heat from internal combustion engine and used optimization process to maximize exergy efficiency and minimize total cost of the system. They also tried to find the best working fluid for ORC cycle. Kim and Perez-Blanco [19] used an organic Rankine cycle and a vapor compression cycle to produce simultaneous power and refrigeration. They also performed a sensitivity analysis on the key parameters of the system, including turbine inlet temperature, turbine inlet pressure, and the flow division ratio. Ebrahimi and Ahookhosh [20] combined a micro gas turbine, an ORC cycle and a steam ejector refrigeration cycle to provide power, heating and cooling simultaneously and defined an objective function based on energy and exergy analyses to optimize the plant. Li et al. [21] analyzed a CCHP system in terms of energy, economic and environment and used weighting method and fuzzy optimum selection theory to optimize the system. They showed that if the system couples with renewable energies and thermal storage systems, performance of the plant increases considerably in all mentioned criteria. Boyaghchi and Heidarnejad [22] performed a thermoeconomic analysis on a solar CCHP system and optimized the plant based on thermal efficiency, exergy efficiency and total product cost rate. Wang et al. [23] integrated a PV-wind system with an internal combustion engine and analyzed the system and provided optimal operation strategy. They also considered the effect of fuel price on the optimal dispatch strategies. Xia et al. [24] coupled solar powered ORC cycle and wind energy to drive a RO system to provide fresh potable water. Cetin et al. [25] studied combination of photovoltaic, wind and fuel cell systems to generate electricity for residential application. Hughes [26] used off-the-shelf electric thermal storage system to provide required heating demand with wind energy. Cavallo [27] showed that utilizing integrated wind-CAES is an affordable strategy for wind generators. Lund and Salgi [28] analyzed the role of CAES system integrated with renewable energies in the future sustainable energy system. They performed their study for Denmark. Kim and Favrat [29] performed energy and exergy analysis on a micro-CAES system coupled with air cycle heating and cooling system. They showed that CAES systems are good candidates for distributed generation systems. Hartmann et al. [30] calculated energy efficiency of different configurations of adiabatic CAES system in a full charge-discharge cycle.

Energy and exergy analyses can be used to provide more information about performance of the system. Ifaei et al. [31,32] proposed two new configurations to reduce water losses in natural draft wet cooling towers in steam power plants. These two configurations are based on integration of steam power plant with vapor compression refrigeration and absorption heat pump. They studied

Please cite this article in press as: Mohammadi A et al. Exergy analysis of a Combined Cooling, Heating and Power system integrated with wind turbine and compressed air energy storage system. Energy Convers Manage (2016), http://dx.doi.org/10.1016/j.enconman.2016.11.003

these cycles in terms of energy, economic, environmental and thermoeconomic analyses. Vandani et al. [33] proposed a new configuration to recover heat from boiler blowdown stream. They used exergy analysis to investigate the effect of the proposed system on the plants performance. Ashouri et al. [34] integrated a parabolic trough collector to a Kalina cycle and studied the system exergetically and economically. Mohammadi and Mehrpooya [35] performed exergy analysis on an integrated system composed of a gas turbine, a dish collector and a CAES system. Cavalcanti and Motta [36] performed exergoeconomic analysis on a solar-powered/fuel assisted Rankine cycle. They performed their study from 7 am to 4 pm at March, June, September and December 21st.

In this paper, a CCHP system is coupled with wind energy and CAES systems to provide cooling, heating and power, simultaneously. The new integrated system has the capability of producing these types of energy during the peak hours in which the energy price is high. Also introducing wind turbines into the system provides the required power for the compressors and therefore net output power of the system increases. Energy and exergy analyses are applied to the system and effects of the key parameters on the system performance are studied using sensitivity analysis.

2. System description

Fig. 1 shows a schematic diagram of the proposed CCHP system. Wind turbines are used to convert kinetic energy of wind into electrical energy. This energy is delivered to the compressors to compress the air. Two compressors are used to provide the required compressed air for the cavern. Since temperature of the cavern is low and near the ambient temperature, an intercooler and an aftercooler are used to recover the heat from compressor exhaust stream and provide hot water for heating purposes. During the peak hours, the compressed air in the cavern is used to drive the gas turbine. Also a combustion chamber is placed prior to the gas turbine to increase temperature of the compressed air. After expansion and producing power, gas turbine outlet stream has still high quality energy which can be used in a bottom cycle. An ORC cycle is used in this paper to recover this heat and produce more power. Therefore, a vapor generator is added to the cycle to produce superheated steam for ORC turbine. To boost efficiency of the cycle, a regenerative ORC cycle is used. Finally, an ammonia-water absorption refrigeration system is placed downstream of the ORC cycle to provide required cooling energy. This absorption chiller can also recover the remaining energy in the flue gas and therefore improve the system efficiency.

It should be noted that there are two trains that operate independently: compression train (before CAES) and expansion train (after the CAES). Compression train includes flows 1–5 and 36–38, whereas expansion train comprises flows 6–35.

3. Mathematical modeling

To analyze the system, energy and exergy balances should be applied to each component. In this section, required equations are presented.

3.1. Energy modeling

The following assumptions are made to simplify the analysis:

- All sections (GT, ORC and chiller) are in steady state condition.
- Air and flue gas are treated as an ideal gas mixture.
- Methane is used as fuel in the combustion chamber.

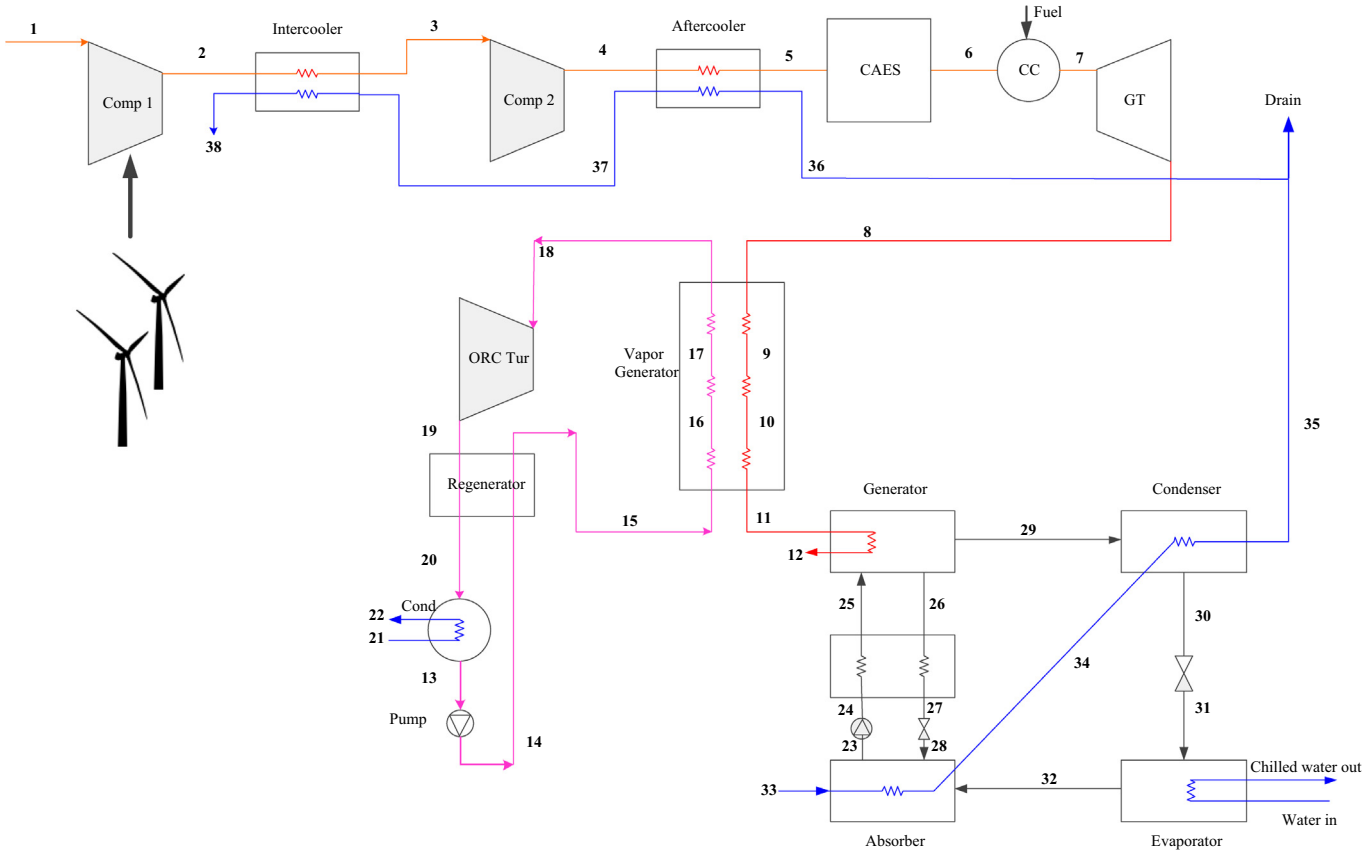

Fig. 1. Schematic diagram of the proposed CCHP system coupled with wind turbine and CAES system.

Please cite this article in press as: Mohammadi A et al. Exergy analysis of a Combined Cooling, Heating and Power system integrated with wind turbine and compressed air energy storage system. Energy Convers Manage (2016), http://dx.doi.org/10.1016/j.enconman.2016.11.003

- The only non-adiabatic component in the system is combustion chamber.
- A constant isentropic efficiency is assumed for compressors, turbines and pumps.
- Generator and evaporator outlet in absorption chiller is assumed to be saturated vapor ammonia.
- Condenser outlet in absorption chiller is assumed to be saturated liquid.

It is assumed that the wind turbines have horizontal shaft, upwind arrangement and three rotor blades. Under these circumstances, power produced by wind turbine can be described as [37]:

$$\dot{W}_{WT} = \frac{c_p \rho A v^3}{2} \tag{1}$$

where c_p is the power coefficient of the turbine and v is velocity of air. This power is transferred to the compressors. The first compressor uses the ambient air as input. Outlet temperature of compressor can be computed using the pressure ratio, isentropic efficiency of the compressor and specific heat ratio of air as follows:

$$T_{out} = T_{in}\left(1 + \frac{1}{\eta_{comp}}\left(r_p^{\frac{\gamma_a - 1}{\gamma_a}} - 1\right)\right) \tag{2}$$

It should be noted that pressure ratio of each compressor is a function of the inlet pressure of the air cavern and can be calculated using the following equation:

$$r_{p1} = r_{p2} = \sqrt{R_p} \tag{3}$$

Having the inlet and outlet temperatures of the compressor, its required power can be estimated as:

$$\dot{W}_{comp} = \dot{m}_a C_{p_a}(T_{out} - T_{in}) \tag{4}$$

Mass flow rate of produced hot water can be computed by applying energy balance for the intercooler and aftercooler, as:

$$\dot{m}_w(h_{out} - h_{in}) = \dot{m}_a C_{p_a}(T_{in} - T_{out}) \tag{5}$$

Mass flow rate of the fuel is obtained using the following equation:

$$\dot{m}_a C_{p_a} T_{in} + \dot{m}_f LHV = \dot{m}_g C_{p_g} T_{out} + (1 - \eta_{CC})\dot{m}_f LHV \tag{6}$$

where η_{CC} is combustion chamber efficiency and LHV is lower heating value of fuel. It should be mentioned that mass flow rate of flue gas is equal to the sum of mass flow rate of air and fuel. Gas turbine outlet temperature can be calculated as:

$$T_{out} = T_{in}\left(1 - \eta_{GT}\left(1 - \left(\frac{P_{in}}{P_{out}}\right)^{\frac{1-\gamma_g}{\gamma_g}}\right)\right) \tag{7}$$

Generated power by gas turbine can be computed as:

$$\dot{W}_{GT} = \dot{m}_g C_{p_g}(T_{in} - T_{out}) \tag{8}$$

It also should be mentioned that charge time and discharge time of the cavern is directly dependent on the air mass flow rate and its density and can be represented as:

$$t_{charge} = \frac{(\rho_5 - \rho_6)V_{storage}}{3600\dot{m}_5} \tag{9}$$

$$t_{discharge} = \frac{(\rho_5 - \rho_6)V_{storage}}{3600\dot{m}_6} \tag{10}$$

Gas turbine outlet stream goes through vapor generator to provide energy for ORC cycle. It has three sections, namely economizer, evaporator and superheater. The following relation should exist between hot and cold stream in the vapor generator based on the pinch concept:

$$T_{16} = T_{10} - pinch_{ORC} \tag{11}$$

Mass flow rate of produced steam in ORC system can be calculated by solving the following equations simultaneously:

$$\dot{m}_g C_{p_g}(T_8 - T_9) = \dot{m}_{ORC}(h_{18} - h_{17}) \tag{12}$$

$$\dot{m}_g C_{p_g}(T_9 - T_{10}) = \dot{m}_{ORC}(h_{17} - h_{16}) \tag{13}$$

$$\dot{m}_g C_{p_g}(T_{10} - T_{11}) = \dot{m}_{ORC}(h_{16} - h_{15}) \tag{14}$$

where Eqs. (12)–(14) represent energy balance for economizer, evaporator and superheater, respectively. In the above equations, $\dot{m}_g$ is constant and equal to mass flow rate of point 8 in Fig. 1. Also energy balance of the recuperator can be written as:

$$\dot{m}_{19}(h_{19} - h_{20}) = \dot{m}_{14}(h_{15} - h_{14}) \tag{15}$$

After calculating thermodynamic properties of all streams in ORC cycle, total generated power in ORC turbine and consumed power in ORC pump can be computed.

$$\dot{W}_{tur} = \dot{m}_{18}(h_{18} - h_{19}) \tag{16}$$

$$\dot{W}_{pump} = \dot{m}_{13}(h_{14} - h_{13}) \tag{17}$$

$$\dot{W}_{ORC} = \dot{W}_{tur} - \dot{W}_{pump} \tag{18}$$

To calculate thermodynamic properties of absorption refrigeration system, concentration balance should be applied to the components, as well as mass balance and energy balance. These equations for generator can be written as:

$$\dot{m}_{25} = \dot{m}_{26} + \dot{m}_{29} \tag{19}$$

$$\dot{m}_{25}x_7 = \dot{m}_{26}x_{26} + \dot{m}_{29} \tag{20}$$

$$\dot{m}_7 h_7 + \dot{m}_{25}h_{25} = \dot{m}_{26}h_{26} + \dot{m}_{29}h_{29} + \dot{m}_{33}h_{33} \tag{21}$$

Using the above equations, mass flow rate of rich and lean solutions can be calculated:

$$\dot{m}_{25} = \frac{1 - x_{26}}{x_{25} - x_{26}}\dot{m}_{29} \tag{22}$$

$$\dot{m}_{26} = \frac{1 - x_{25}}{x_{25} - x_{26}}\dot{m}_{29} \tag{23}$$

Performance of the heat exchanger is evaluated using a constant parameter named effectiveness which is defined as:

$$\epsilon = \frac{T_{27} - T_{26}}{T_{24} - T_{26}} \tag{24}$$

Also energy balance of the heat exchanger is as follows:

$$\dot{m}_{24}(h_{25} - h_{24}) = \dot{m}_{26}(h_{26} - h_{27}) \tag{25}$$

Energy balance for absorber, evaporator and condenser are expressed as:

$$\dot{m}_{32}h_{32} + \dot{m}_{33}h_{33} + \dot{m}_{28}h_{28} = \dot{m}_{23}h_{23} + \dot{m}_{34}h_{34} \tag{26}$$

$$\dot{m}_{31}h_{31} - \dot{m}_{32}h_{32} = \dot{Q}_{cooling} \tag{27}$$

$$\dot{m}_{29}h_{29} + \dot{m}_{34}h_{34} = \dot{m}_{30}h_{30} + \dot{m}_{35}h_{35} \tag{28}$$

Besides, energy consumption of chiller pump is computed as:

$$\dot{W}_{pump,chiller} = \dot{m}_{23}(h_{24} - h_{23}) \tag{29}$$

Please cite this article in press as: Mohammadi A et al. Exergy analysis of a Combined Cooling, Heating and Power system integrated with wind turbine and compressed air energy storage system. Energy Convers Manage (2016), http://dx.doi.org/10.1016/j.enconman.2016.11.003

Finally coefficient of performance for the absorption refrigeration system is defined as:

$$COP = \frac{\dot{m}_{31}(h_{31} - h_{32})}{\dot{W}_{pump,ref} + \dot{m}_{11}(h_{11} - h_{12})} \quad (30)$$

Table 1 shows the value of constant parameters used in the mathematical modeling of the system.

3.2. Exergy modeling

After applying first law of thermodynamics to each component and calculating thermodynamic properties of each stream, exergy analysis can be done. To do this, exergy balance should be applied to each component which is defined as:

$$\dot{E}x^{Q} + \sum \dot{m}_{in} ex_{in} = \dot{E}x^{w} + \sum \dot{m}_{out} ex_{out} + \dot{E}x^{D} \quad (31)$$

In this equation, $\dot{E}x^{Q}$ and $\dot{E}x^{w}$ are exergy associated to heat and power, respectively. Also $\dot{E}x^{D}$ is exergy destruction of the component. Finally ex is specific exergy of each stream which is equal to the sum of its physical and chemical exergies as follows:

$$ex = ex_{ph} + ex_{ch} \quad (32)$$

$$ex_{ph} = (h - h_0) - T_0(s - s_0) \quad (33)$$

$$ex_{ch} = \sum_{i=1}^{N} y_i ex_i^{ch} + RT_0 \left(\sum_{i=1}^{N} y_i ln(y_i) \right) \quad (34)$$

Also exergy of fuel can be computed using the following empirical equation:

$$\xi = \frac{ex_{fuel}}{LHV_{fuel}} \quad (35)$$

where the value of ξ is close to unity. Using the above equations, exergy destruction of each component can be calculated. Table 2 lists required equations to compute exergy destruction and efficiency of each component.

Table 1
Constant parameters of the cycle.

Parameter	Unit	Value
Ambient temperature	C	25
Ambient pressure	bar	1.01
Number of wind turbines	–	4
Average wind speed	m/s	4.8
Power coefficient	–	0.45
Volume of air cavern	m^3	300
Maximum pressure of air cavern	bar	10
Minimum pressure of air cavern	bar	7
Cavern inlet mass flow rate	kg/s	0.096
Cavern outlet mass flow rate	kg/s	0.06
Compressor isentropic efficiency	%	85
Combustion chamber efficiency	%	95
Turbine isentropic efficiency	%	85
Turbine inlet temperature	C	800
LHV of fuel	kJ/kg	48,000
Pinch temperature in vapor generator	C	10
ORC turbine inlet temperature	C	350
ORC turbine inlet pressure	bar	25
Condenser pressure	bar	0.1
ORC turbine isentropic efficiency	%	80
ORC pump isentropic efficiency	%	70
Recuperator pinch	C	10
Maximum pressure of chiller	bar	20.33
Minimum pressure of chiller	bar	4.7
Concentration of strong solution	%	43
Concentration of weak solution	%	26
Heat exchanger effectiveness	%	80

Table 2
Exergy destruction of each component in the cycle [38,39].

Component	Exergy destruction	Exergy efficiency
Wind turbine	$\dot{E}x^{D}_{wind} = \left(\frac{1}{c_p} - 1\right)\dot{W}_{WT}$	$\psi_{wind} = \frac{\dot{W}_{WT}}{\dot{E}x_{WT}}$
Compressor	$\dot{E}x^{D}_{comp} = \dot{E}x_{in} - \dot{E}x_{out} + \dot{W}_{AC}$	$\psi_{comp} = \frac{\dot{E}x_{out} - \dot{E}x_{in}}{\dot{W}_{comp}}$
Heat exchanger	$\dot{E}x^{D}_{HRSG} = \sum \dot{E}x_{in} - \sum \dot{E}x_{out}$	$\psi_{HRSG} = \frac{(\dot{E}x_{out} - \dot{E}x_{in})_{cold}}{(\dot{E}x_{in} - \dot{E}x_{out})_{hot}}$
CAES	$\dot{E}x^{D}_{CAES} = \dot{E}x_{in} - \dot{E}x_{out}$	$\psi_{CAES} = 1 - \frac{\dot{E}x^{D}_{CAES}}{\dot{E}x_{in}}$
Combustion chamber	$\dot{E}x^{D}_{CC} = \dot{E}x_{in} + \dot{E}x_{fuel} - \dot{E}x_{out}$	$\psi_{CC} = \frac{\dot{E}x_{out} - \dot{E}x_{in}}{\dot{E}x_{fuel}}$
Turbine	$\dot{E}x^{D}_{Tur} = \dot{E}x_{in} - \dot{E}x_{out} - \dot{W}_{GT}$	$\psi_{Tur} = \frac{\dot{W}_{Tur}}{\dot{E}x_{in} - \dot{E}x_{out}}$
Vapor generator	$\dot{E}x^{D}_{VG} = \sum \dot{E}x_{in} - \sum \dot{E}x_{out}$	$\psi_{VG} = \frac{(\dot{E}x_{out} - \dot{E}x_{in})_{cold}}{(\dot{E}x_{in} - \dot{E}x_{out})_{hot}}$
Condenser	$\dot{E}x^{D}_{cond} = \sum \dot{E}x_{in} - \sum \dot{E}x_{out}$	$\psi_{cond} = \frac{(\dot{E}x_{out} - \dot{E}x_{in})_{cold}}{(\dot{E}x_{in} - \dot{E}x_{out})_{hot}}$
Pump	$\dot{E}x^{D}_{pump} = \dot{E}x_{in} - \dot{E}x_{out} + \dot{W}_{Pump}$	$\psi_{pump} = \frac{\dot{E}x_{out} - \dot{E}x_{in}}{\dot{W}_{pump}}$

3.3. Performance criteria

Since the compression and expansion trains work in different times, simple first law efficiency cannot be defined for this system. Another parameter named round trip efficiency (RTE) is defined which is the ratio of total energy output, including electrical, thermal and cooling energy to the total energy input in a full charge/discharge cycle. This formula is expressed as [39]:

$$\text{RTE} = \frac{E_{elec,net} + E_{heat} + E_{cooling}}{E_{fuel} + E_{elec}} \quad (36)$$

Another parameter to evaluate the cycle is total exergy destruction which can be defined as:

$$\dot{E}x^{D}_{tot} = sum(\dot{E}x^{D}) \quad (37)$$

4. Validation

The proposed system in this paper is a new and novel cycle and it has not been constructed in reality. Therefore to validate the model, each section has been validated separately and the results are presented in Table 3. Since error percent in each subsection is quite low, therefore it could be concluded that the model is accurate.

5. Results and discussion

A simulation program has been developed in Matlab software to analyze the system. Thermodynamic properties of all fluids are calculated using REFPROP [43]. Table 4 lists thermodynamic properties of each stream of the cycle. Since the operation of compression and expansion trains does not occur simultaneously, the corresponding flows have been separated.

Using the above data and equations in Section 3, performance indicators of the cycle can be calculated. As can be seen in Table 5, under design conditions, it takes 2.88 h for the compressors to fill the cavern, while its discharge time is equal to 4.61 h. Usually peak hours are last for 3–5 h; therefore the proposed system could be matched well to fulfill the energy requirement. Also power production by wind turbines is 28.87 kW which is almost equal to the required power by compressors. ORC turbine can produce almost 30% of the power produced by gas turbine using its exhaust stream. Finally, the system has the capacity of producing 2.56 kW cooling with COP of 65.86% and 1.82 ton of hot water per day which can be used for heating purposes. In general, round trip efficiency of the system is equal to 53.94% and its total exergy destruction is 133.35 kW. As can be seen, round trip efficiency of the proposed

Please cite this article in press as: Mohammadi A et al. Exergy analysis of a Combined Cooling, Heating and Power system integrated with wind turbine and compressed air energy storage system. Energy Convers Manage (2016), http://dx.doi.org/10.1016/j.enconman.2016.11.003

Table 3
Comparison between obtained results and data published in other literatures [40–42].

Parameter		Present work	Reference	Error (%)
Brayton cycle	Gas turbine power output (MW)	95.08	94.423	0.69
	Gas turbine outlet temperature (C)	532.2	532.4	0.04
	Fuel mass flow (kg/s)	6.80	6.72	1.19
Organic Rankine cycle	Produced mass flow rate (kg/s)	82.90	82.31	0.72
	Evaporator outlet temperature (C)	110.54	110.36	0.16
	ORC turbine outlet temperature (C)	60.82	61.33	0.83
Refrigeration system	Heat load in generator (kW)	275.07	275.07	0
	Heat load in evaporator (kW)	63.22	62.7	0.83
	COP	0.23	0.227	1.32

Table 4
Thermodynamic properties of each stream of the cycle.

State	Fluid	P [bar]	T [C]	h [kJ/kg]	s [kJ/kg K]	m [kg/s]	ex [kJ/kg]
Compression train							
1	Air	1.01	25	302.856	6.886	0.096	3.634
2	Air	3.19	161.73	447.614	6.938	0.096	132.976
3	Air	3.16	40	319.247	6.605	0.096	103.896
4	Air	10	184.44	474.335	6.659	0.096	242.902
5	Air	10	40	322.356	6.268	0.096	207.459
36	Water	1.01	33.25	139.418	0.481	0.175	0.469
37	Water	1.01	53.19	222.743	0.745	0.175	5.242
38	Water	1.01	70	293.122	0.955	0.175	12.923
Expansion train							
6	Air	7	40	320.992	6.373	0.060	174.824
7	Flue gas	7	800	1250.395	7.692	0.061	693.793
8	Flue gas	1.04	462.37	820.9	7.745	0.061	248.534
9	Flue gas	1.04	381.07	713.673	7.589	0.061	187.839
10	Flue gas	1.03	290.57	604.408	7.457	0.061	117.831
11	Flue gas	1.02	160.16	449.777	7.072	0.061	77.996
12	Flue gas	1.01	100	386.495	7.030	0.061	27.454
13	Toluene	0.1	45.25	-123.115	-0.351	0.037	1.043
14	Toluene	26.03	46.62	-118.721	-0.347	0.037	4.203
15	Toluene	25.77	180.26	149.958	0.351	0.037	65.046
16	Toluene	25.51	280.57	406.782	0.860	0.037	169.983
17	Toluene	25.25	279.81	588.258	1.188	0.037	253.582
18	Toluene	25	350	766.350	1.493	0.037	340.927
19	Toluene	0.1	227.96	560.537	1.598	0.037	103.607
20	Toluene	0.1	56.64	291.859	0.952	0.037	27.669
21	Water	1.01	25	104.920	0.367	0.366	0
22	Water	1.01	35	146.720	0.505	0.366	0.686
23	Ammonia-water	4.7	47.61	114.623	1.133	0.006	8611.677
24	Ammonia-water	20.33	47.93	117.320	1.136	0.006	8613.622
25	Ammonia-water	20.33	100.74	367.951	1.858	0.006	8648.935
26	Ammonia-water	20.33	144.34	552.397	2.157	0.004	5477.604
27	Ammonia-water	20.33	67.21	194.237	1.210	0.004	5401.854
28	Ammonia-water	4.7	67.48	194.237	1.215	0.004	5400.287
29	Ammonia	20.33	49.98	1634.229	5.521	0.003	409.682
30	Ammonia	20.33	49.98	583.675	2.270	0.003	328.466
31	Ammonia	4.7	2.44	583.675	2.344	0.003	306.411
32	Ammonia	4.7	2.44	1607.962	6.061	0.003	222.564
33	Water	1.01	25	104.920	0.367	0.193	0
34	Water	1.01	30	125.822	0.437	0.193	0.173
35	Water	1.01	33.25	139.418	0.481	0.193	0.469

system is lower than the data available in [39] which is due to utilization of renewable energy in the proposed system.

Table 6 shows exergy destruction of each component along with their share in total exergy destruction and their exergy efficiency. As can be seen, wind turbines are responsible for more than 60 percent of total exergy destruction in the system. This is because 4 wind turbines are used in the system and each of them has its own irreversibilities. After wind turbines, combustion chamber has the highest rate of exergy destruction with 27.56 kW which is due to combustion reaction and heat transfer to the ambient. Also CAES has the third rank in exergy destruction. These three components are responsible for almost 90% of total exergy destruction in the cycle, while other components have a negligible share. It should be mentioned that between ORC components, the turbine has the highest share, while in absorption chiller system this role belongs to the generator.

5.1. Parametric analysis

To analyze the sensitivity of the system to its parameters, a parametric analysis has been performed in this section. To do so, only the parameter under study changes and all the other parameters are kept constant.

5.1.1. Effect of maximum pressure of air cavern

Fig. 2 shows the effect of maximum pressure of air cavern on the system performance. This parameter can only affect the compression train. As a result, power generated and cooling capacity

Please cite this article in press as: Mohammadi A et al. Exergy analysis of a Combined Cooling, Heating and Power system integrated with wind turbine and compressed air energy storage system. Energy Convers Manage (2016), http://dx.doi.org/10.1016/j.enconman.2016.11.003

Table 5
Results of the simulation program.

Parameter	Unit	Value
Charge time	Hour	2.88
Discharge time	Hour	4.61
$\dot{W}_{wind}$	kW	28.87
$\dot{W}_{comp1}$	kW	13.89
$\dot{W}_{comp2}$	kW	14.88
$\dot{W}_{GT}$	kW	26.27
$\dot{W}_{ORC_{tur}}$	kW	7.58
$\dot{W}_{ORC_{pump}}$	kW	0.16
$\dot{W}_{REF_{pump}}$	kW	0.02
$\dot{m}_{fuel}$	kg/s	0.0012
$\dot{Q}_{eva}$	kW	2.56
$\dot{m}_{hot_{water}}$	Ton/day	1.82
COP	%	65.86
RTE	%	53.94
$\dot{E}x_{D,tot}$	kW	133.35

Table 6
Exergy destruction and share and exergy efficiency of each component in the cycle.

Component	Exergy destruction (kW)	Share of exergy destruction (%)	Exergy efficiency (%)
Wind turbine	82.55	61.91	0.43
Compressor 1	1.48	1.11	0.89
Intercooler	1.45	1.08	0.48
Compressor 2	1.54	1.16	0.90
Aftercooler	2.57	1.92	0.25
CAES	9.43	7.07	0.53
Combustion chamber	27.56	20.67	0.54
Gas turbine	0.96	0.72	0.94
Vapor generator	0.27	0.20	0.96
ORC turbine	1.16	0.87	0.87
Regenerator	0.56	0.42	0.80
ORC condenser	0.73	0.55	0.26
ORC pump	0.05	0.03	0.72
Chiller condenser	0.17	0.13	0.28
Valve 1	0.07	0.05	–
Evaporator	0.01	0.01	0.39
Absorber	0.59	0.44	0.18
Chiller pump	0.01	0.00	0.71
Valve 2	0.01	0.01	–
Heat exchanger	0.15	0.11	0.57
Generator	2.05	1.54	0.39

do not change with variation of this parameter, because they are related to expansion train. When, maximum pressure of air cavern increases, power consumption by compressors rises, while power production by expansion train remains constant. On the other hand, both charge and discharge time of the system increases due to increase in density of air at the inlet of cavern which enables the system to operate for longer hours (as shown in Fig. 3). This results in increasing round trip efficiency of the system. Also pressure increment results in higher exergy destruction in compressors and CAES systems. Therefore total exergy destruction of the system increases.

With increasing pressure ratio of the compressors, their outlet temperature increases. Consequently more energy is available in intercooler and after cooler to produce hot water which increases mass flow rate of produced hot water (Fig. 3).

5.1.2. Effect of minimum pressure of air cavern

Unlike the previous case, variation of minimum pressure of air cavern can affect the expansion train. Increasing this parameter increases power generated by gas turbine due to increasing its pressure ratio. Also based on Eq. (7) by increasing this parameter, outlet temperature of gas turbine decreases. Therefore lower amount of energy is available for ORC cycle to recover and this reduces power generated by ORC turbine. In general, RTE increases and total exergy destruction of the system decreases with increasing minimum pressure of air cavern as shown in Fig. 4.

This parameter can also affect charge and discharge time of the system as shown in Fig. 5. Both these parameters decrease with increasing minimum pressure of air cavern due to decreasing density of outlet air from the cavern. Also due to lower heat recovery in ORC cycle, delivered heat to generator in chiller increases which raises cooling capacity of the system.

5.1.3. Effect of caverns outlet air mass flow rate

Figs. 6 and 7 show variation of system performance with changing caverns outlet mass flow rate. Increasing this parameter leads to higher power production by gas turbine and ORC turbine (Fig. 6). On the other hand, since discharge time of the system decreases as shown in Fig. 7, in general, RTE of the system remains almost unchanged. Furthermore, increasing mass flow rate increases total exergy destruction of the system.

When caverns outlet mass flow rate increases, more energy is delivered into the bottom cycles, including ORC cycle and absorption chiller. This increases cooling capacity of the system which itself increases COP of the chiller.

5.1.4. Effect of gas turbine inlet temperature

Fig. 8 represents the effect of changing gas turbine inlet temperature on system performance. Increasing gas turbine inlet temperature increases power generated by gas turbine. On the other hand, based on Eq. (7), gas turbine outlet temperature also increases.

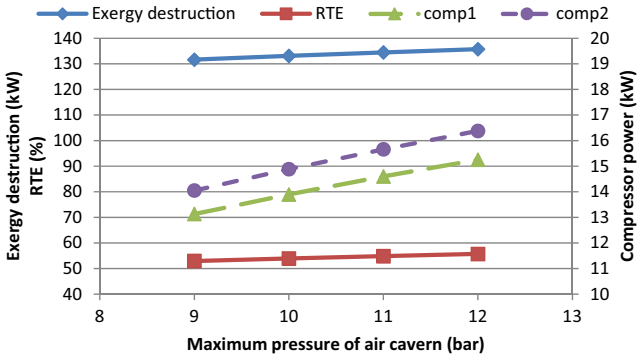

Fig. 2. Variation of total exergy destruction, RTE and compressor power by maximum pressure of air cavern.

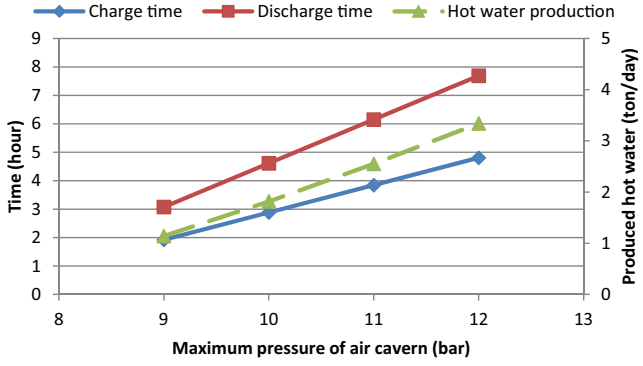

Fig. 3. Variation of charge and discharge time and hot water production with maximum pressure of air cavern.

Please cite this article in press as: Mohammadi A et al. Exergy analysis of a Combined Cooling, Heating and Power system integrated with wind turbine and compressed air energy storage system. Energy Convers Manage (2016), http://dx.doi.org/10.1016/j.enconman.2016.11.003

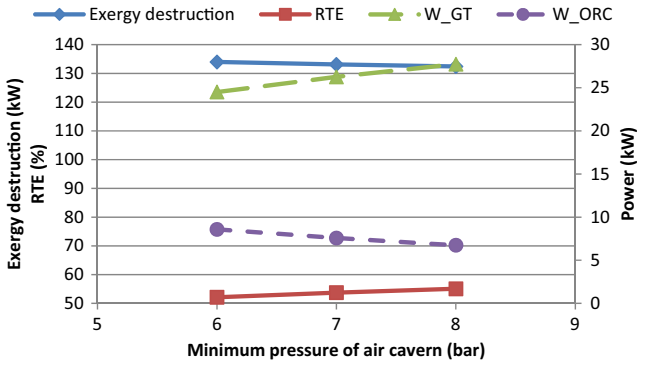

Fig. 4. Variation of system performance with changing minimum pressure of air cavern.

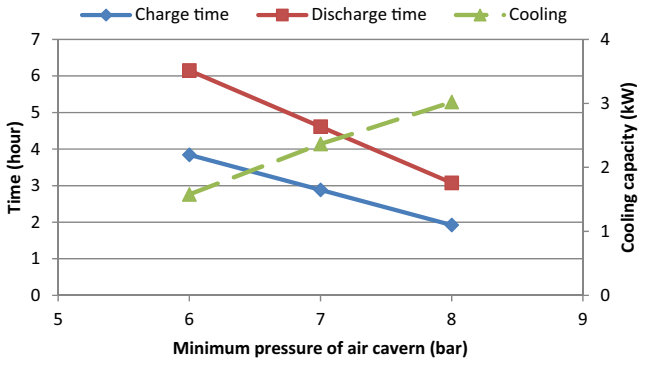

Fig. 5. Variation of operating hour of the system along with its cooling capacity with changing minimum pressure of air cavern.

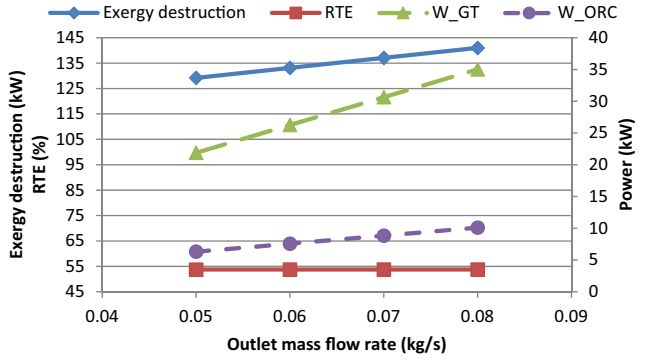

Fig. 6. Variation of system performance with changing mass flow rate of caverns outlet.

Therefore more energy is delivered to the ORC cycle and consequently generated power by ORC cycle increases. To increase gas turbine inlet temperature, more fuel should be burned in combustion chamber. As a result, total exergy destruction of the system increases. In this condition, both power generated and fuel consumption are increasing, but the effect of fuel consumption is higher and therefore RTE decreases slightly. With increasing gas turbine inlet temperature and consequently increasing gas turbine outlet temperature, heat recovery in ORC cycle increases. Therefore lower amount of energy is delivered to the chiller which reduces its cooling capacity as shown in Fig. 8.

5.1.5. Effect of ORC turbine inlet temperature

Fig. 9 shows the effect of ORC turbine inlet temperature on system performance. ORC cycle is placed downstream of the gas turbine, therefore any changes in its operating parameters do not change power generated by gas turbine. When ORC turbine inlet temperature increases, enthalpy of this stream increases too. But on the other hand, mass flow rate of produced organic fluid decreases which results in lower power generated by ORC turbine. It also results in lower heat recovery in ORC cycle and therefore delivered heat into the chiller and cooling capacity of the system increases. In general, increasing this parameter leads to an increment in both exergy destruction and RTE of system.

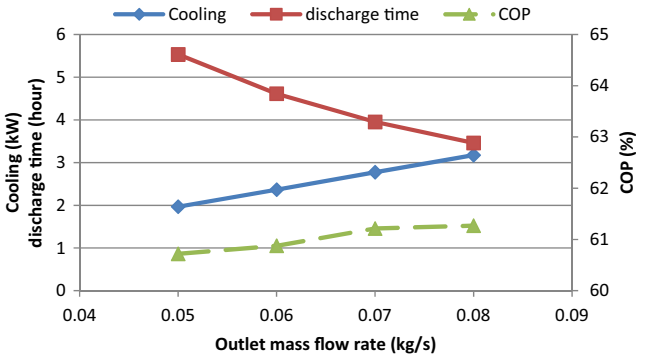

Fig. 7. Changing discharge time and chiller performance with changing caverns outlet mass flow rate.

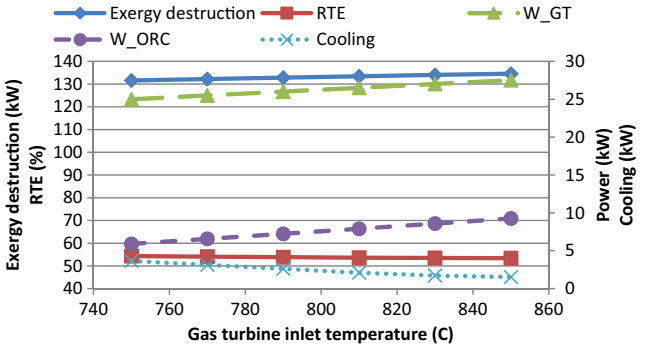

Fig. 8. Variation of system performance with changing gas turbine inlet temperature.

5.1.6. Effect of turbine inlet pressure

Fig. 10 shows the effect of ORC turbine inlet pressure on system performance. With increasing ORC turbine inlet pressure and therefore changing turbine inlet enthalpy, higher amount of organic fluid will be produced in vapor generator. Consequently,

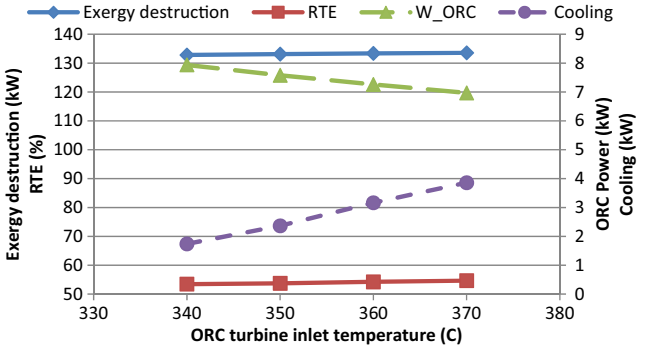

Fig. 9. Variation of system performance with changing ORC turbine inlet temperature.

Please cite this article in press as: Mohammadi A et al. Exergy analysis of a Combined Cooling, Heating and Power system integrated with wind turbine and compressed air energy storage system. Energy Convers Manage (2016), http://dx.doi.org/10.1016/j.enconman.2016.11.003

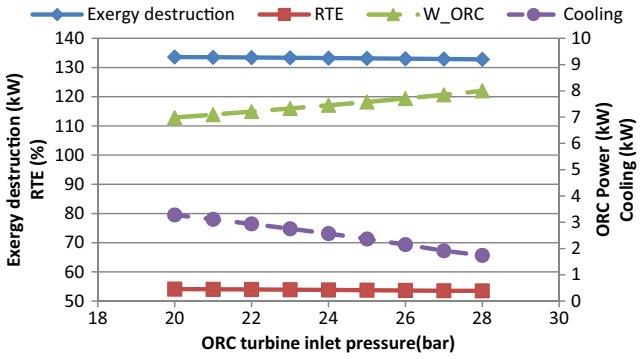

Fig. 10. Variation of system performance with changing ORC turbine inlet pressure.

ORC power production increases. Like other cases, with increasing heat recovery in ORC cycle cooling capacity in chiller reduces. As shown in the figure, increasing ORC turbine inlet pressure reduces both total exergy destruction and RTE of the system slowly. Compared to the previous case, this parameter has lower impact on total exergy destruction and round trip efficiency.

5.1.7. Effect of vapor generator pinch temperature

Fig. 11 shows the effect of vapor generator pinch temperature on system performance. Lower pinch temperature means higher heat recovery in vapor generator. Consequently, with increasing pinch temperature, heat recovery in ORC cycle decreases which results in lower power production in ORC turbine. Also this results in higher amount of heat delivery into refrigeration system which leads to increment in cooling capacity of the system. In general, increasing pinch temperature slightly increases both total exergy destruction and RTE of the system. It also increases COP of the chiller slightly.

5.1.8. Effect of minimum pressure of chiller

Fig. 12 shows the effect of minimum pressure of chiller on system performance. This parameter only affects chillers performance and does not cause any changes on the upstream components. As can be seen, the higher the minimum pressure, the higher the cooling capacity. It also increases exergy destruction in chiller which itself increases total exergy destruction in the system, while round trip efficiency of the system changes insignificantly.

5.1.9. Effect of maximum pressure of chiller

Fig. 13 represents changes in system performance with variation of maximum pressure of chiller. Like the previous case, this parameter only can affect chillers performance. Cooling capacity of chiller reduces with increasing maximum pressure of chiller. This is due to reduction in ammonia mass flow rate in generator. It also increases total exergy destruction of system slightly, while round trip efficiency reduces.

5.1.10. Effect of heat exchangers effectiveness

Fig. 14 shows variation of system performance with heat exchangers effectiveness. This parameter only affects chillers performance and with increasing effectiveness of the heat exchanger, cooling capacity of absorption chiller increases. This is due to higher heat transfer in heat exchanger which results in production of higher amount of ammonia in chiller. Also total exergy destruction and round trip efficiency of the system remain almost unchanged.

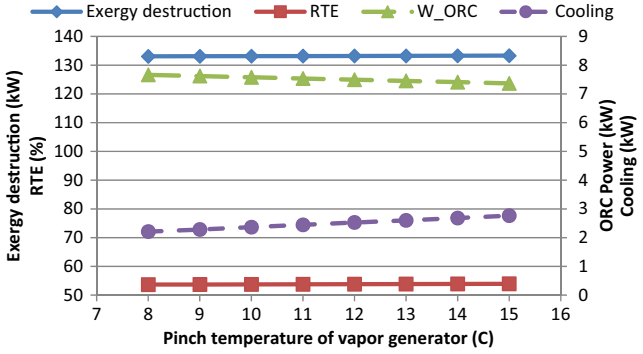

Fig. 11. Variation of system performance with changing pinch temperature of vapor generator.

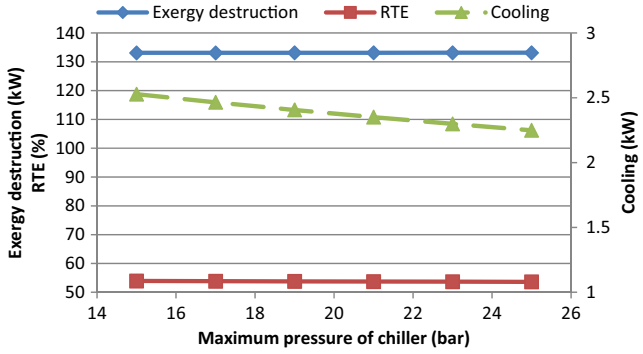

Fig. 13. Variation of system performance with changing maximum pressure of chiller.

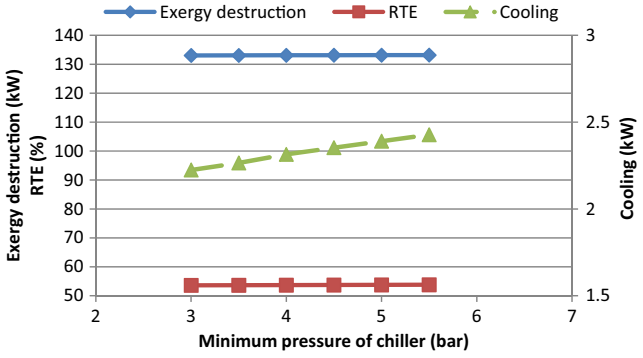

Fig. 12. Variation of system performance with changing minimum pressure of chiller.

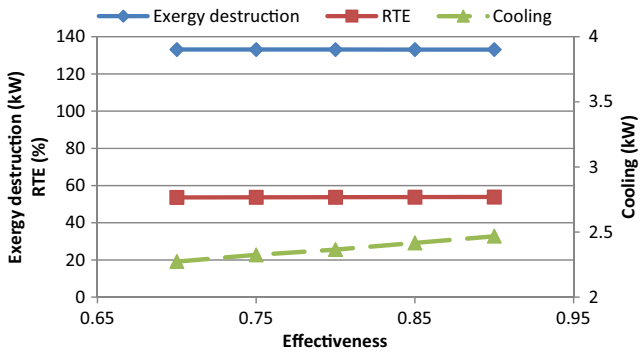

Fig. 14. Variation of system performance with changing heat exchangers effectiveness.

Please cite this article in press as: Mohammadi A et al. Exergy analysis of a Combined Cooling, Heating and Power system integrated with wind turbine and compressed air energy storage system. Energy Convers Manage (2016), http://dx.doi.org/10.1016/j.enconman.2016.11.003

6. Conclusion

A wind turbine, a CAES system and a CCHP system are integrated in this paper to produce cooling, heating and power simultaneously using renewable energies. Energy and exergy analyses are carried out to investigate performance of the system based on first and second laws of thermodynamics. Also a sensitivity analysis is conducted to evaluate the effects of these parameters on system performance. The main conclusions are summarized as follows:

- The obtained results showed that the proposed system is a good candidate to be used in residential sector. Because it benefits from renewable energy and it also can provide different kinds of energy (cooling, heating and power). It also helps to reduce energy consumption during peak hours.
- Under design conditions, the system is capable of producing 33.67 kW power, 2.56 kW cooling and 1.82 ton hot water per day with a round trip efficiency of 53.94%. To do this, the system uses energy provided by wind turbines (83.24 kW h) and fuel combustion (258.97 kW h).
- Results of exergy analysis showed that highest exergy destruction occur in wind turbines, combustion chamber and CAES system, respectively.
- Sensitivity analysis showed that increasing the difference between maximum and minimum pressure air cavern increases round trip efficiency and total exergy destruction of the system. It also has been concluded that since gas turbine, ORC cycle and refrigerator systems are cascaded to each other, any changes in one of these systems, will cause a change in other systems.

References

[1] International Energy Outlook 2007. United States Department of Energy, Washington, DC; Retrieved 6 June 2007.
[2] Cho H, Smith AD, Mago P. Combined cooling, heating and power: a review of performance improvement and optimization. Appl Energy 2014;136:168–85.
[3] Hanafizadeh P et al. Evaluation and sizing of a CCHP system for a commercial and office buildings. J Build Eng 2016;5:67–78.
[4] Chen X et al. Performance analysis of 5 kW PEMFC-based residential micro-CCHP with absorption chiller. Int J Hydrogen Energy 2015;40(33):10647–57.
[5] Ma S et al. Thermodynamic analysis of a new combined cooling, heat and power system driven by solid oxide fuel cell based on ammonia–water mixture. J Power Sources 2011;196(20):8463–71.
[6] Zhao H, Jiang T, Hou H. Performance analysis of the SOFC–CCHP system based on H_2O/Li–Br absorption refrigeration cycle fueled by coke oven gas. Energy 2015;91:983–93.
[7] Li Y, Hu R. Exergy-analysis based comparative study of absorption refrigeration and electric compression refrigeration in CCHP systems. Appl Therm Eng 2016;93:1228–37.
[8] Ebrahimi M, Keshavarz A, Jamali A. Energy and exergy analyses of a micro-steam CCHP cycle for a residential building. Energy Build 2012;45:202–10.
[9] Gao P et al. Thermodynamic performance assessment of CCHP system driven by different composition gas. Appl Energy 2014;136:599–610.
[10] Chen Q et al. The exergy and energy level analysis of a combined cooling, heating and power system driven by a small scale gas turbine at off design condition. Appl Therm Eng 2014;66(1):590–602.
[11] Moya M et al. Performance analysis of a trigeneration system based on a micro gas turbine and an air-cooled, indirect fired, ammonia–water absorption chiller. Appl Energy 2011;88(12):4424–40.
[12] Ochoa AAV et al. Energetic and exergetic study of a 10RT absorption chiller integrated into a microgeneration system. Energy Convers Manage 2014;88:545–53.
[13] Yang C et al. Analytical off-design characteristics of gas turbine-based CCHP system. Energy Proc 2015;75:1126–31.
[14] Kong X, Wang R, Huang X. Energy optimization model for a CCHP system with available gas turbines. Appl Therm Eng 2005;25(2):377–91.
[15] Borunda M et al. Organic Rankine Cycle coupling with a Parabolic Trough Solar Power Plant for cogeneration and industrial processes. Renewable Energy 2016;86:651–63.
[16] Pantaleo AM, Camporeale S, Fortunato B. Small scale biomass CHP: techno-economic performance of steam vs gas turbines with bottoming ORC. Energy Proc 2015;82:825–32.
[17] Fang F et al. Complementary configuration and operation of a CCHP-ORC system. Energy 2012;46(1):211–20.
[18] Javan S et al. Fluid selection optimization of a combined cooling, heating and power (CCHP) system for residential applications. Appl Therm Eng 2016;96:26–38.
[19] Kim KH, Perez-Blanco H. Performance analysis of a combined organic Rankine cycle and vapor compression cycle for power and refrigeration cogeneration. Appl Therm Eng 2015;91:964–74.
[20] Ebrahimi M, Ahookhosh K. Integrated energy–exergy optimization of a novel micro-CCHP cycle based on MGT–ORC and steam ejector refrigerator. Appl Therm Eng 2016;102:1206–18.
[21] Li M et al. Optimal design and operation strategy for integrated evaluation of CCHP (combined cooling heating and power) system. Energy 2016;99:202–20.
[22] Boyaghchi FA, Heidarnejad P. Thermoeconomic assessment and multi objective optimization of a solar micro CCHP based on organic Rankine cycle for domestic application. Energy Convers Manage 2015;97:224–34.
[23] Wang J, Wu J, Zheng C. Design and operation of a hybrid CCHP system including PV-Wind devices. In: ASME 2013 international mechanical engineering congress and exposition. American Society of Mechanical Engineers; 2013.
[24] Xia G et al. Theoretical analysis of a reverse osmosis desalination system driven by solar-powered organic Rankine cycle and wind energy. Desalination Water Treat 2015;53(4):876–86.
[25] Cetin E et al. A micro-DC power distribution system for a residential application energized by photovoltaic–wind/fuel cell hybrid energy systems. Energy Build 2010;42(8):1344–52.
[26] Hughes L. Meeting residential space heating demand with wind-generated electricity. Renewable Energy 2010;35(8):1765–72.
[27] Cavallo A. Controllable and affordable utility-scale electricity from intermittent wind resources and compressed air energy storage (CAES). Energy 2007;32(2):120–7.
[28] Lund H, Salgi G. The role of compressed air energy storage (CAES) in future sustainable energy systems. Energy Convers Manage 2009;50(5):1172–9.
[29] Kim YM, Favrat D. Energy and exergy analysis of a micro-compressed air energy storage and air cycle heating and cooling system. Energy 2010;35(1):213–20.
[30] Hartmann N et al. Simulation and analysis of different adiabatic compressed air energy storage plant configurations. Appl Energy 2012;93:541–8.
[31] Ifaei P, Ataei A, Yoo C. Thermoeconomic and environmental analyses of a low water consumption combined steam power plant and refrigeration chillers-part 2: thermoeconomic and environmental analysis. Energy Convers Manage 2016;123:625–42.
[32] Ifaei P, Rashidi J, Yoo C. Thermoeconomic and environmental analyses of a low water consumption combined steam power plant and refrigeration chillers – part 1: energy and economic modelling and analysis. Energy Convers Manage 2016;123:610–24.
[33] Vandani AMK, Bidi M, Ahmadi F. Exergy analysis and evolutionary optimization of boiler blowdown heat recovery in steam power plants. Energy Convers Manage 2015;106:1–9.
[34] Ashouri M et al. Techno-economic assessment of a Kalina cycle driven by a parabolic Trough solar collector. Energy Convers Manage 2015;105:1328–39.
[35] Mohammadi A, Mehrpooya M. Exergy analysis and optimization of an integrated micro gas turbine, compressed air energy storage and solar dish collector process. J Clean Prod 2016;139:372–83.
[36] Cavalcanti EJC, Motta HP. Exergoeconomic analysis of a solar-powered/fuel assisted Rankine cycle for power generation. Energy 2015;88:555–62.
[37] Stiebler M. Wind energy systems for electric power generation. Springer Science & Business Media; 2008.
[38] Ozlu S, Dincer I. Development and analysis of a solar and wind energy based multigeneration system. Sol Energy 2015;122:1279–95.
[39] Zhao P, Dai Y, Wang J. Performance assessment and optimization of a combined heat and power system based on compressed air energy storage system and humid air turbine cycle. Energy Convers Manage 2015;103:562–72.
[40] Raghuvanshi S, Maheshwari G. Analysis of ammonia-water (NH_3-H_2O) vapor absorption refrigeration system based on first law of thermodynamics. Int J Sci Eng Res 2011;2(8):1.
[41] Rašković P, Guzović Z, Cvetković S. Performance analysis of electricity generation by the medium temperature geothermal resources: Velika Ciglena case study. Energy 2013;54:11–31.
[42] Vandani AMK, Joda F, Boozarjomehry RB. Exergic, economic and environmental impacts of natural gas and diesel in operation of combined cycle power plants. Energy Convers Manage 2016;109:103–12.
[43] Lemmon EW, Huber ML, McLinden MO. NIST reference fluid thermodynamic and transport properties–REFPROP; 2002 [version].

Please cite this article in press as: Mohammadi A et al. Exergy analysis of a Combined Cooling, Heating and Power system integrated with wind turbine and compressed air energy storage system. Energy Convers Manage (2016), http://dx.doi.org/10.1016/j.enconman.2016.11.003